*Acta Cryst.* (1994). A**50**, 33–45

# On the Average Coulomb Potential ($\Phi_0$) and Constraints on the Electron Density in Crystals

BY M. O'KEEFFE

*Department of Chemistry, Arizona State University, Tempe, AZ 85287, USA*

AND J. C. H. SPENCE

*Department of Physics and Astronomy, Arizona State University, Tempe, AZ 85287, USA*

(*Received* 16 *December* 1992; *accepted* 10 *May* 1993)

## Abstract

The rôle of the average Coulomb potential (mean inner potential), $\Phi_0$, in electron diffraction and methods for its calculation are reviewed. From an examination of model and real crystals, it is shown that a prescription of Becker & Coppens [*Acta Cryst.* (1990), A**46**, 254–258] for calculating the average potential from X-ray data may lead to incorrect results because of an artificial surface-dipole term that is independent of crystal size. It is suggested that measurements of $\Phi_0$ for crystals with adsorbed monolayers could be used to measure the density and sign of a real surface dipole moment. Published data for MgO, silicon and aluminium show that $\Phi_0$ is very sensitive to bonding effects when atoms combine to form crystals. The often-reported expansion of the silicon valence shell deduced from pseudo-atom refinements of X-ray diffraction data is shown to be an artifact of the refinement method, as recent accurate measurements of $\Phi_0$ for silicon instead require a contraction of the outer part of the valence shell. It is concluded that X-ray diffraction data alone do not allow a determination of $\Phi_0$. However, $\Phi_0$ provides information about valence-electron distributions that is not available in practice from X-ray data and places powerful constraints on pseudo-atom refinements.

## 1. Introduction

It is widely accepted that, whereas X-ray diffraction techniques probe the electronic part of the total ground-state charge density $\rho(\mathbf{r})$ in a crystal, high-energy electrons are diffracted by the electrostatic (Coulomb) potential $\varphi(\mathbf{r})$, which is related to $\rho(\mathbf{r})$ by Poisson's equation. Considerable interest attaches to reconciliation of the results of these two types of experiment. Recently, attention has been focused on the average electrostatic potential (also called the 'mean inner potential'), $\Phi_0$, which can be determined by electron interferometry (Spence, 1993). In particular, the question has been raised as to whether $\Phi_0$ can be determined from the results of X-ray experiments (Becker & Coppens, 1990).

That the subject is not entirely uncontroversial is illustrated by the fact that it is common in solid-state physics to set the average potential of a periodic charge distribution to zero (see §3 below). In early work that attempted to correlate electron diffraction data and X-ray diffraction data, the average potential was also set equal to zero (*e.g.* Laschkarew & Tschaban, 1935). A similar practice is sometimes followed by crystallographers (*e.g.* Spackman & Stewart, 1981) interested in mapping out the electrostatic-potential distributions in crystals. In a recent theoretical study of crystalline MgO (Saunders, Freyria-Fava, Dovesi, Salasco & Roetti, 1992), the zero of potential was chosen to correspond to that at a point midway between the Mg and O atoms.

Confusion also sometimes arises because electronic-band-structure theorists use the term 'potential' to include an exchange-correlation potential in addition to the electrostatic (Coulomb or Hartree) potential. Many authors use the symbol $V_0$ for $\Phi_0$ but, since it is also common to use the symbol $V$ for a related quantity with different dimensions, it seems better to avoid that usage. In real crystals, $\Phi_0$ is a positive quantity, usually measured in V. The potential energy of an electron caused by this potential is $\mathbf{e}\Phi_0$ (where $\mathbf{e}$ is the electron charge $-e$) and is negative.

In this paper, we argue that the average potential in a finite crystal is a well defined quantity, but that extending the concept to an *infinite* crystal can lead to incorrect conclusions. We also show that $\Phi_0$ contains valuable information about bonding effects that occur when atoms combine to form crystals. Accordingly, after some preliminary remarks, we examine some prescriptions for calculating the average potential and apply them first to model systems and then to MgO, silicon and aluminium, for which appropriate experimental and/or theoretical data are




ISSN 0108-7673 

available. As the subject has a long history, we first review some of the key early work, which appears to be in danger of being forgotten.

An electron entering a crystal is accelerated by the mean inner potential ($\Phi_0$) and therefore undergoes a phase shift with respect to a reference beam in a vacuum. For this reason, $\Phi_0$ contributes to a 'refractive index' for electrons different from unity and played an important role in the early history of electron diffraction and quantum mechanics. Because the directions of Bragg maxima in reflection electron diffraction (RED) experiments depend on refraction, the experimental confirmation of de Broglie's matter-wave hypothesis by Davisson & Germer (1927) required a knowledge of $\Phi_0$. Lacking this information, they were, therefore, unable to index the reflections in their famous RED patterns. The slightly later high-energy work of Thomson & Reid (1927) was not so affected because they used the transmission geometry.

With its importance recognized, the first theory of the mean inner potential was given by Bethe (1928), who expressed $\Phi_0$ in terms of the second moment of the charge density [equation (9) below] for spherical atoms. Values of $\Phi_0$ were subsequently measured for many crystals in Europe and in Japan by electron optical methods and a summary of early results was given by Thomson & Cochrane (1939). A summary of the many measurements made on MgO up to 1973 was given by Yada, Shibata & Hibi (1973) and a review of recent data was given by Spence (1993). It should be noted that many of the early results have large uncertainties associated with factors such as uncertainties in sample thickness and surface contamination. Electron-holography measurements on cleavage wedges, which avoid many of the systematic errors in previous work, have recently been made (Gajdardziska-Josifovska, McCartney, de Ruijter, Smith, Weiss & Zuo, 1993) and accuracies of the order of 1% are possible. Representative results, to which we refer later, are given in Table 1. Note that these experiments are transmission experiments so they do not sample only surface layers of the crystal but instead measure a bulk property. In Table 1, we also give the value of $\Phi_0$ calculated for a superposition of free atoms (the pro-crystal discussed below); note that these are substantially higher than the crystal values.

Rosenfeld (1929) first related $\Phi_0$ to the diamagnetic susceptibility and this relationship has since been used to estimate $\Phi_0$ (Miyake, 1940) and the electron scattering factor at zero scattering angle (Ibers, 1958). Bethe's expression for $\Phi_0$ was recast in the form of a sum over certain X-ray structure factors by Shinohara (1932) [see also Miyake (1940)]. This idea, that $\Phi_0$ forms a kind of sum rule on X-ray structure factors, is discussed briefly in Appendix *A*.

Table 1. *The mean Coulomb potential in crystals (in* V*) measured (Gajdardziska-Josifovska et al., 1993) by electron holography*

The measured values are corrected for multiple scattering. Values calculated for a pro-crystal of noninteracting atoms are given for comparison.

| | Crystal | Pro-crystal |
|---|---|---|
| Silicon | 9.26 (8) | 13.61 |
| MgO | 13.01 (8) | 18.43 |
| GaAs | 14.53 (17) | 15.32 |
| PbS | 17.19 (12) | |

The proposal that $\Phi_0$ should approximately equal the sum of the magnitudes of the Fermi kinetic energy and the work function in photo-emission was apparently also first made by Bethe (1928) [see also Tamm (1932) and Kisliuk (1961)]. A review of the theory of the work function and its relationship to $\Phi_0$ has been given by Lang & Kohn (1971).

It is important to recognize that in high-energy ($>50$ kV) electron diffraction (HEED) it is well established (Rez, 1978) that exchange between the beam electrons and the crystal-electrons is negligible. This implies (Yoshioka, 1957) that the total wave function $\Psi(\mathbf{r},\mathbf{r}_i)$, dependent on the high-energy electron coordinates $\mathbf{r}$ and the crystal-electron coordinates $\mathbf{r}_i$, can be written as a product of a crystal-electron wave function $\Psi_c$ and a beam-electron wave function $\Psi_b$: $\Psi(\mathbf{r},\mathbf{r}_i) = \Psi_c(\mathbf{r}_i)\Psi_b(\mathbf{r})$. In this (excellent) approximation, the potential seen by the beam electron is just the Coulomb potential in the crystal (the Hartree potential) and does not include exchange and correlation terms. The situation is quite different in low-energy electron diffraction (LEED) where estimates of $\Phi_0$ are subject to a number of important corrections (exchange and correlation effects) not present at higher beam energies.

We wish to point out also that Bragg's law fails under conditions of strong multiple electron scattering. Thus, 'dynamical shifts' occur in the positions of Bragg peaks for both transmission and reflection electron diffraction (Spence & Zuo, 1992). The Renninger effect (*e.g.* Chang, 1987) is the corresponding X-ray multiple scattering effect. These shifts depend in general on all the strongly excited electron structure factors, including that for zero-angle scattering, so that it is no longer possible to treat the refractive index for electrons simply in terms of $\Phi_0$. A treatment of the Bloch-wave Bethe theory for reflection high-energy electron diffraction (RHEED), with emphasis on the problem of determining $\Phi_0$, is given by Stern & Gervais (1969). In this work, a value of $\Phi_0 = 20$ V is obtained for tungsten, for example, which is in reasonable agreement with the value of 23.4 V obtained by the analysis of Kikuchi patterns at higher voltages by Gaukler & Schwarzer (1971).

In what follows, we discuss some general charge distributions but point out that a charge distribution in a real crystal is far from arbitrary, being, to a very good first approximation, that of a superposition of free spherical atoms. Following common practice, we refer to this approximation as the 'pro-crystal'. An even better approximation is that of a superposition of pseudo-atoms [*e.g.* Dawson (1967), Stewart (1973) and Hansen & Coppens (1978)] whose charge distributions are refined to match observed structure factors.

## 2. Charge density and potential and their Fourier representations

In this work, for reasons that will become apparent, we deal only with finite charge distributions. We start from the definition that the potential resulting from an element of charge $q$ at a distance $r$ from the charge is $\varphi = q/r$, so that $\varphi \rightarrow 0$ as $r \rightarrow \infty$; this defines the zero of potential. The potential at a point $\mathbf{R}$ resulting from a finite charge distribution $\rho(\mathbf{r})$, such that $\int \rho(\mathbf{r}) \mathrm{d}\tau = 0$, is then the volume integral over all of direct space $\mathbf{r}$:

$$\varphi(\mathbf{R}) = \int \rho(\mathbf{r})/|\mathbf{r} - \mathbf{R}| \mathrm{d}\tau. \tag{1}$$

The Fourier transforms of $\rho(r)$ and $\varphi(r)$ are

$$f(\mathbf{k}) = \int \rho(\mathbf{r}) \exp(2\pi i \mathbf{k} \cdot \mathbf{r}) \mathrm{d}\tau, \tag{2}$$

$$v(\mathbf{k}) = \int \varphi(\mathbf{r}) \exp(2\pi i \mathbf{k} \cdot \mathbf{r}) \mathrm{d}\tau. \tag{3}$$

These quantities are related by Poisson's equation in reciprocal space $\mathbf{k}$:

$$v(\mathbf{k}) = f(\mathbf{k})/\pi k^2. \tag{4}$$

In particular,

$$v(0) = \int \varphi(\mathbf{r}) \mathrm{d}\tau = \lim_{k \rightarrow 0} \{\langle f(k) \rangle / \pi k^2\}. \tag{5}$$

As $v(0)$ is a scalar quantity, we replace $f(\mathbf{k})$ in (4) by its orientational average $\langle f(k) \rangle$ in (5) (*cf.* Becker & Coppens, 1990). From (2), we have, explicitly, with spherical polar coordinates $k$, $\theta$, $\varphi$:

$$\begin{aligned} \langle f(k) \rangle &= (1/4\pi) \int_0^{\pi} \int_0^{2\pi} \int \rho(\mathbf{r}) \exp(2\pi i \mathbf{k} \cdot \mathbf{r}) \mathrm{d}\tau \, \mathrm{d}\varphi \sin\theta \, \mathrm{d}\theta \\ &= (1/4\pi) \int \rho(\mathbf{r}) \int_0^{\pi} \int_0^{2\pi} \exp(2\pi i \mathbf{k} \cdot \mathbf{r}) \mathrm{d}\varphi \sin\theta \, \mathrm{d}\theta \, \mathrm{d}\tau \\ &= \int \rho(\mathbf{r}) [\sin(2\pi k r)/2\pi k r] \mathrm{d}\tau. \end{aligned} \tag{6}$$

Using the expansion for small $x$ of $\sin(x)/x = 1 - x^2/6 + O(x^4)$ and recalling that $\int \rho(\mathbf{r}) \mathrm{d}\tau = 0$, we get, for small $k$,

$$\langle f(k) \rangle = (-2\pi^2 k^2/3) \int r^2 \rho(\mathbf{r}) \mathrm{d}\tau + O(k^4). \tag{7}$$

And thus, from (5),

$$v(0) = (-2\pi/3) \int r^2 \rho(\mathbf{r}) \mathrm{d}\tau. \tag{8}$$

We see that $v(0)$ is simply related to the second moment of $\rho(r)$. We note also that (8) applied to an atom of atomic number $Z$ (noting that electron charge is negative) gives the celebrated Bethe (1928) formula:

$$v(0) = 2\pi Z \langle r^2 \rangle / 3. \tag{9}$$

It is also useful to observe that $v(0)$ is simply related to the curvature of $\langle f(k) \rangle$ at the origin. Specifically, from (5), we have, directly, a result we refer to later:

$$v(0) = (-1/2\pi) [\mathrm{d}^2 \langle f(k) \rangle / \mathrm{d}k^2]_{k=0}. \tag{10}$$

## 3. The potential in a finite crystal

We now turn to a discussion of a finite crystal (or *crystallite*). A finite element of an infinite lattice $Z(\mathbf{r})$ may be represented as $z(\mathbf{r}) = Z(\mathbf{r}) s(\mathbf{r})$, where $s(\mathbf{r})$, equal to unity inside the crystallite and zero outside, is a shape function. Now we make a crystallite by associating a basis with each of the finite number of lattice points. A given charge distribution in the interior of the crystallite can be described by an infinite number of different bases. An important result, apparently first established by Harris (1975), is that, provided the basis has zero dipole and quadrupole moments, the potentials calculated using different bases differ only by a constant amount everywhere inside a crystallite of arbitrary shape. In what follows, we demonstrate this result for two particularly important bases, although a more general treatment is straightforward (*e.g.* Saunders *et al.*, 1992). We then argue that one of these bases is the appropriate choice for a real crystal and that the potential calculated on this basis has the correct average, $\Phi_0$.

The first choice of basis is the contents of a unit cell $\rho_c(\mathbf{r})$ and the second choice is a unit cell of pseudo-atoms $\rho_{ai}(\mathbf{r}_i)$, where $\mathbf{r}_i$ is the position of the $i$th pseudo-atom in the unit cell. Note that the pseudo-atom charge densities may, and in general will, extend beyond the boundary of the unit cell. The two representations of the charge density are given by the convolutions

$$\rho_1(\mathbf{r}) = z(\mathbf{r}) * \rho_c(\mathbf{r}), \tag{11a}$$

$$\rho_2(\mathbf{r}) = z(\mathbf{r}) * \sum_i \rho_{ai}(\mathbf{r} - \mathbf{r}_i). \tag{11b}$$

These charge densities are identical in an infinite crystal but will differ at the surfaces of a crystallite.

Let $\zeta(\mathbf{k})$ be the Fourier transform of $z(\mathbf{r})$. $\zeta(0)$ is just the number $N$ of lattice points in the crystallite. Likewise, let $f_c(\mathbf{k})$ and $f_{ai}(\mathbf{k})$ be the Fourier transforms of $\rho_c(\mathbf{r})$ and $\rho_{ai}(\mathbf{r})$, respectively. The Fourier

transforms of the charge distributions in (11) are

$$F_1(\mathbf{k}) = \zeta(\mathbf{k})f_c(\mathbf{k}), \tag{12a}$$

$$F_2(\mathbf{k}) = \zeta(\mathbf{k})\sum_i f_{ai}(\mathbf{k}) \exp(2\pi i\mathbf{k}\cdot\mathbf{r}_i). \tag{12b}$$

The Fourier transforms of the potential due to the two charge distributions are

$$V_1(\mathbf{k}) = \zeta(\mathbf{k})f_c(\mathbf{k})/\pi k^2, \tag{13a}$$

$$V_2(\mathbf{k}) = \zeta(\mathbf{k})\sum_i f_{ai}(\mathbf{k}) \exp(2\pi i\mathbf{k}\cdot\mathbf{r}_i)/\pi k^2. \tag{13b}$$

In particular, recalling that $\zeta(0) = N$,

$$V_1(0) = Nv_c(0), \tag{14a}$$

$$V_2(0) = N\sum_i v_{ai}(0). \tag{14b}$$

For a large (neutral) crystallite made up of $N$ unit cells of volume $\Omega$ and for which the potential falls rapidly to zero outside, the average potential in the crystallite is $V(0)/N\Omega$:

$$\Phi_{01} = v_c(0)/\Omega, \tag{15a}$$

$$\Phi_{02} = \sum_i v_{ai}(0)/\Omega. \tag{15b}$$

From (8) we finally get

$$\Phi_{01} = (-2\pi/3\Omega)\int_{\text{cell}} r^2\rho_c(\mathbf{r})\mathrm{d}\mathbf{r}, \tag{16a}$$

$$\Phi_{02} = (-2\pi/3\Omega)\sum_i\left[\int_{\text{pseudo-atom}} r^2\rho_{ai}(\mathbf{r})\mathrm{d}\mathbf{r}\right]. \tag{16b}$$

The first of these prescriptions for calculating the average potential is equation (29) of Becker & Coppens (1990), the second is implied in their equation (38). It is important to notice, however, that the Becker & Coppens results were derived for an 'infinite' crystal, whereas our treatment is for a finite crystallite of arbitrary shape. We now first show, using simple examples, that the two expressions (16*a*) and (16*b*) can lead to very different results and then analyze the reasons for the difference.

Consider a crystallite composed of point nuclei of charge $Z$ neutralized by a spherical Gaussian distribution of negative charge with $\langle r^2\rangle = b^2 = 3\eta^2/2$ at each lattice point. Specifically,

$$\rho_a(\mathbf{r}) = Z[\delta(\mathbf{r}) - (\eta\pi^{1/2})^{-3}\exp(-r/\eta)^2], \tag{17}$$

$$\varphi_a(\mathbf{r}) = Z\,\mathrm{erfc}(\eta r)/r \tag{18}$$

$$v_a(0) = Z\pi\eta^2. \tag{19}$$

In (18), $\mathrm{erfc}(z) = 1 - \mathrm{erf}(z)$ is the complementary error function.

The crystallite is now composed of pseudo-atoms such as these centered on the points of a primitive cubic lattice parameter $a$. We have, immediately, by substitution of (19) into (15*b*),

$$\Phi_{02} = Z\pi\eta^2/a^3. \tag{20}$$

As $b$ approaches infinity, the negative charge density in the crystal approaches the constant value $-Z/a^3$ and we have a lattice of point positive charges neutralized by a uniform negative charge; an abstraction frequently encountered in solid-state physics ('Wigner crystal'). Note that in the same limit, (20) shows that the average potential will go to infinity. This observation led to the conclusion that the average potential in a periodic charge distribution must be zero (Fuchs, 1935; Ewald & Juretschke, 1953; Tosi, 1964) [but see also von Laue (1948)]. In fact, of course, such a charge distribution is unphysical and would only be found as an infinite energy excitation of a crystal.

In this limit ($b\to\infty$), the charge density in the unit cell is $Z[\delta(\mathbf{r}) - 1/a^3]$ and we find from (16*a*) that $\Phi_{01}$ becomes independent of $\eta$:

$$\Phi_{01} = Z\pi/6a. \tag{21}$$

In the other limit, that of $b$ approaching zero, $\Phi_{01} = \Phi_{02} = Z\pi\eta^2/a^3$ and it is clear that the two bases only give the same result for a crystallite made up of nonoverlapping pseudo-atoms. Fig. 1 shows the ratio of $\Phi_{01}$ to $\Phi_{02}$ calculated from (16) as a function of $b/a$. The two methods only agree for $b$ [$=\langle r^2\rangle^{1/2}$] less than about $a/4$. Note for future reference that the charge distribution in a unit cell is taken as that in a unit cell of an infinite crystal.

The question naturally arises of how important the distinction between $\Phi_{01}$ and $\Phi_{02}$ is for real atoms. Fig. 2 shows the ratio $\Phi_{01}/\Phi_{02}$ for primitive cubic pro-crystals of sodium, magnesium, silicon and oxygen as functions of the lattice parameter $a$. It can be seen that the two values converge only for rather large lattice constants for the electropositive atoms. For these calculations (and all other calculations of

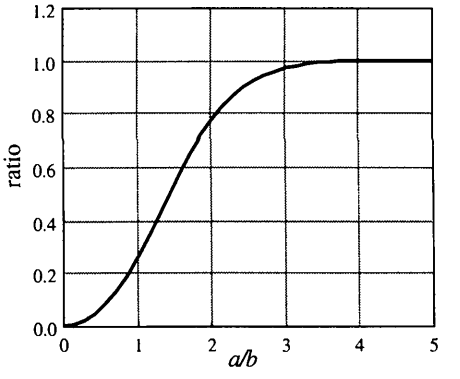


Fig. 1. The ratio $\Phi_{01}/\Phi_{02}$ calculated [from (16)] for a cubic crystal of Gaussian pseudo-atoms as a function of the ratio of the lattice parameter $a$ and the r.m.s. width of the Gaussians $b$.

atomic properties reported below) we have used the atomic wave functions of Clementi & Roetti (1974).

It is important to recognize that $f_c(\mathbf{k})$ and $f_a(\mathbf{k})$ are only equal for $\mathbf{k}=\mathbf{H}$ (a reciprocal-lattice vector) and likewise that $f_c(\mathbf{0}) = f_a(\mathbf{0}) = 0$. Fig. 3 shows $f_c(\mathbf{k})$ and $f_a(\mathbf{k})$ along the direction $[\mathbf{k}_x,0,0]$ for a cubic crystal of Gaussian pseudo-atoms for a particular choice of width parameter $\eta = 0.2a$. The curves intersect only at reciprocal-lattice vectors and, in particular, have different curvatures at the origin.

For $\mathbf{H}\neq 0$, we also have $v_c(\mathbf{H}) = v_a(\mathbf{H})$, but $v_c(0)$ and $v_a(0)$ will not be equal as they will depend on the curvatures of $f_c(\mathbf{k})$ and $f_a(\mathbf{k})$ at the origin [(10)]. Fig. 4 shows $v_c(\mathbf{k})$ and $v_a(\mathbf{k})$ for the same crystal as in Fig. 3. The curves intersect for nonzero reciprocal-lattice vectors so that $f_c(\mathbf{H}) = f_a(\mathbf{H})$ but $v_c(0) \neq v_a(0)$.

If one does a Fourier synthesis of $f(\mathbf{H})$,

$$\rho(\mathbf{r}) = (1/\Omega)\sum_{\mathbf{H}} f(\mathbf{H}) \exp(-2\pi i \mathbf{H}\cdot\mathbf{r}), \qquad (22)$$

the same charge density in a unit cell of an 'infinite' crystal will be obtained using either $f_c(\mathbf{k})$ or $f_a(\mathbf{k})$. On the other hand, if one does a Fourier synthesis of $v(\mathbf{H})$, including $v(0)$,

$$\varphi(\mathbf{r}) = (1/\Omega)\sum_{\mathbf{H}} v(\mathbf{H}) \exp(-2\pi i \mathbf{H}\cdot\mathbf{r}), \qquad (23)$$

potential distributions will be obtained that are the same except for a constant difference $\Delta\Phi_0 = [v_c(0) - v_a(0)]/\Omega$. We now show that $\Delta\Phi_0$ is a surface contribution that arises from the different ways of terminating the crystal and is independent of its size (or shape), so one cannot go to the limit of infinite size to evaluate the potential distribution in a crystal in this way. We should mention that this conclusion was reached earlier by Kleinman (1981) for a Wigner crystal.

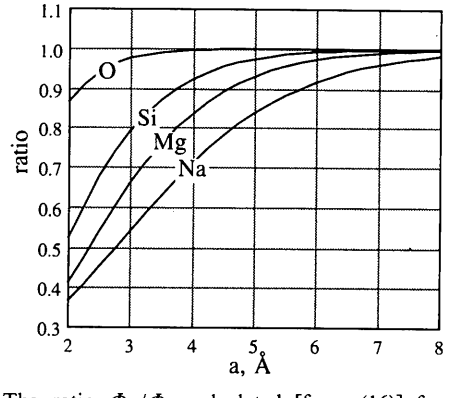


Fig. 2. The ratio $\Phi_{01}/\Phi_{02}$ calculated [from (16)] for a cubic pro-crystal of Hartree–Fock atoms as a function of the lattice parameter $a$ (Å).

## 4. The surface dipole contribution to $\Phi_0$

To demonstrate the effect of surface charges on $\Phi_0$ in a crystallite, we use an example of a crystallite having *only* surface charges. The total charge distribution is still described by the methods of §3, *i.e.* we still associate a charge distribution with every point in a finite element of a lattice. Specifically, we now use as basis for a crystallite a distribution of charge:*

$$\rho(\mathbf{r}) = 6q\rho_s(\mathbf{r}) - \sum_{i=1}^{6} q\rho_s(\mathbf{r}-\mathbf{r}_i), \qquad (24)$$

where $\rho_s(r)$ is a normalized and spherically symmetric charge distribution $[f_s(0) = 1]$ and the $\mathbf{r}_i$ are $\pm a,0,0$; $0,\pm a,0$; $0,0,\pm a$. The Fourier transform of this basis is

$$f(\mathbf{k}) = 6qf_s(\mathbf{k}) - \sum_{i=1}^{6} qf_s(\mathbf{k}) \exp(-2\pi i \mathbf{k}\cdot\mathbf{r}_i). \qquad (25)$$

It may readily be verified that (5) and (8) give the same result:

$$v(0) = 4\pi q a^2. \qquad (26)$$

* We are grateful to O. F. Sankey for suggesting this example; an octahedral distribution of point charges was discussed by Harris (1975).

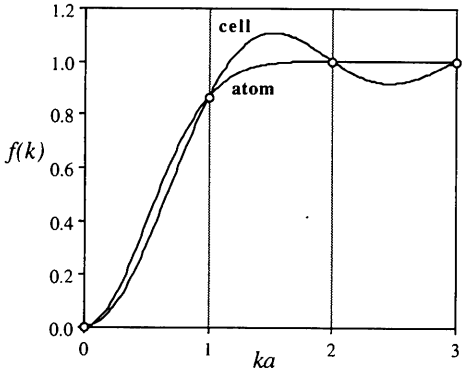


Fig. 3. $f_c(\mathbf{k})$('cell') and $f_a(\mathbf{k})$('atom') along $\mathbf{k}_x,0,0$ for a cubic crystal (lattice parameter $a$) of Gaussian pseudo-atoms with $\eta = 0.2a$.

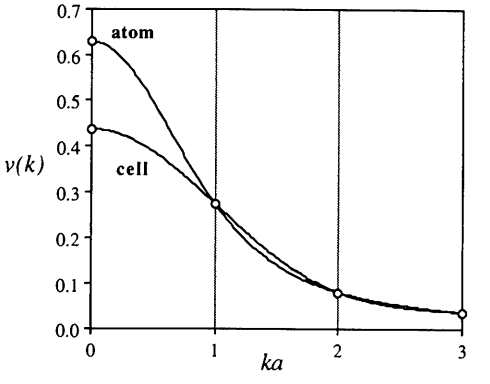


Fig. 4. $v_c(\mathbf{k})$('cell') and $v_a(\mathbf{k})$('atom') in units of $ea^2$ along $\mathbf{k}_x,0,0$ for the same crystal as in Fig. 3.

Note that the actual functional form of $\rho_s(r)$ is irrelevant to $v(0)$.

If we make an infinite crystal by associating the octahedral basis with every lattice point of a primitive cubic lattice of cell edge $a$, then associated with every lattice point $\mathbf{r}_l$ is a charge density $6q\rho(\mathbf{r}_l) - 6q\rho(\mathbf{r}_l) = 0$, *i.e.* we have a null crystal for which one would naturally assign $\Phi_0 = 0$. On the other hand, if we make a finite crystal with the same basis we find [*cf.* (15*b*)]

$$\Phi_0 = v(0)/\Omega = 4\pi q/a. \tag{27}$$

This average potential is independent of crystallite size or shape and, as the charge is zero everywhere inside and outside the crystallite, must be due to the residual charges on the surface. Fig. 5 shows a layer of a crystallite built up from the octahedral basis and shows that there is a dipole layer at the surface. The shaded area in the figure represents a square prism of side $a$ normal to one of the surfaces and might be taken to represent the trajectory of an electron traversing the crystal.

It is again convenient for numerical work to use Gaussian charge distributions (but now without a neutralizing point charge, as in the pseudo-atoms of §3) to construct the overall-neutral octahedral basis. Specifically, we use in (24)

$$\rho_s(\mathbf{r}) = (\eta\pi^{1/2})^{-3}\exp(-r/\eta)^2, \tag{28}$$

with the properties $f(0) = 1$, $\varphi(r) = \operatorname{erf}(r/\eta)/r$, $\varphi(0) = 2/\pi^{1/2}\eta$.

In Fig. 6, we show the potential averaged over the area of a prism of side $a$ as a function of distance from the center for a crystallite constructed from the octahedral basis employing such Gaussians. It is to be noted that inside the crystallite the potential is very nearly constant, is effectively independent of the parameter $\eta$ and drops very close to zero outside the dipole layer.

This result is not entirely unexpected. For a charge distribution consisting of an arbitrary closed surface with constant dipole-moment density $D$ on the surface, it can be shown (*e.g.* Jackson, 1975) that the electrostatic potential everywhere inside is larger by $4\pi D$ than the potential outside. $D$ is considered positive if the dipoles are oriented so that the positive end is inside the surface. It is instructive to derive this result for a crystallite using the methods of this paper.

Consider a cubic crystallite of side $l$ with $n$ dipoles per unit area on the surface, so that the total number of dipoles is $6nl^2$. Let the dipole consist of a charge $q$ at a distance $[(l/2)^2 + i^2 + j^2]^{1/2}$ from the center (here $i$ and $j$ are coordinates on the surface) and $-q$ at a distance $[(l/2 + \delta l)^2 + i^2 + j^2]^{1/2}$ from the center. The second moment of the charge distribution in the dipole layers is

$$\begin{aligned}\omega &= 6nl^2q[l^2/4 - (l/2 + \delta l)^2] \\ &\simeq -6nl^3q\delta l \\ &= -6l^3D,\end{aligned} \tag{29}$$

where on the second line we neglect $\delta l$ compared to $l$ (this corresponds to the limit of point dipoles) and $D = nq\delta l$ is the dipole moment per unit area. As the potential is essentially uniform inside the crystallite and falls essentially to zero outside (*cf.* Fig. 6), we can equate $\Delta\Phi_0$ for the crystallite to $V(0)/l^3$ and, from (8), we have, for the contribution from the dipole layer to $\Phi_0$:

$$\Delta\Phi_0 = -2\pi\omega/3l^3 = 4\pi D. \tag{30}$$

We can now see why the two bases of §3 gave different values for $\Phi_0$ [(16)]. Fig. 7 compares the

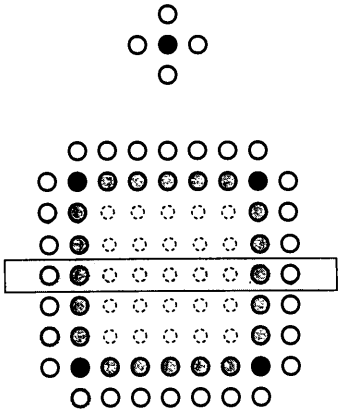

Fig. 5. Top: A layer of an octahedral charge distribution. Filled circle = $6q$, open circles = $-q$. Bottom: A layer of a crystallite made by repeating the octahedral charge distribution. Open circles = $-q$, lightly shaded circles = $+q$, heavier shaded circles = $+2q$.

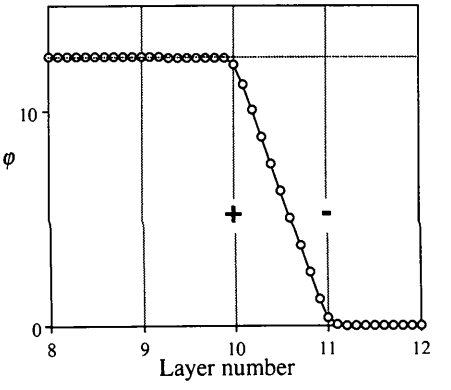


Fig. 6. The potential (in units of $q/a$), averaged over a square of side $a$, normal to the face of a crystallite such as that in Fig. 5. The crystallite is made from $21 \times 21 \times 21$ units of an octahedral basis of Gaussian charges with $\eta = 0.2a$. The dipole layer is between layers 10 and 11. The dotted line corresponds to $\varphi = 4\pi q/a$.

charge distributions for the two. The unit-cell description differs from the pseudo-atom description by a dipole layer that is positive on the outside and this gives a negative dipole-layer contribution to $\Phi_0$, resulting in a lower value than that calculated for the pseudo-atom basis, *i.e.* $\Phi_{01} < \Phi_{02}$. As the dipole-layer term is independent of size, it will remain if one attempts to go to the limit of 'infinite' size.

A real crystal terminates in atoms, rather than by an abrupt discontinuity in electron density, so the pseudo-atom description of (16*b*) is more appropriate than the unit-cell description (16*a*). In general, the surfaces of crystals are not expected to be highly polarized and we make an order-of-magnitude estimate of $\Delta\Phi_0$ for a real crystal as follows. The density of atoms on a surface is typically 0.1–0.2 $Å^{-2}$. If we make the generous estimate that associated with each surface atom there is a dipole moment of $0.1e \times 0.1$ Å, we have $D = 0.015$–$0.03$ V and $\Delta\Phi_0 = 0.2$–$0.4$ V; of the order of magnitude of experimental accuracy. Note that a layer 3 Å thick with $D = 0.03$ V corresponds to a polarization of 0.01 C $m^{-2}$, fairly typical of that found for ferroelectrics (Jona & Shirane, 1962). In what follows, we assume that the surface contribution $\Delta\Phi_0 = 0$ and use (15*b*) to evaluate $\Phi_0$ for a pro-crystal or crystal, as is common practice.

However, we call attention to the possibility of substantial dipole layers occurring on the surfaces of crystals in certain circumstances. Thus, if there were a monolayer of atoms of very different electronegativity adsorbed on all the surface of a crystallite at low temperatures, the surface dipole moment could easily be very much larger than that estimated above and easily measurable effects should be found.

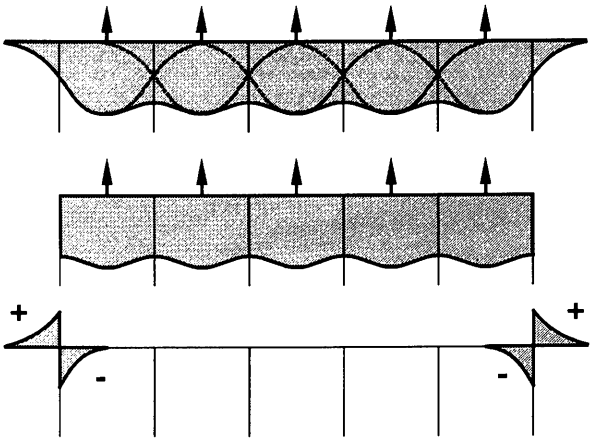


Fig. 7. Comparison of two ways of assembling a crystallite from bases. Top: charge density in a crystallite of pseudo-atoms. Middle: the charge density as an assembly of unit cells. Bottom: the difference showing the surface dipole layer. The arrows indicate the positions of the nuclei of the pseudo-atoms.

We suggest, therefore, that measurements of $\Phi_0$ could be a useful tool for surface scientists. Recall that $\Delta\Phi_0$ depends on the sign of the surface dipoles.

## 5. $\Phi_0$ in real crystals: MgO, silicon and aluminium

### *Magnesium oxide*

There have been numerous measurements of $\Phi_0$ for MgO by electron interferometry (Spence, 1993). Recently, an accurate value of 13.01 V, not subject to the experimental uncertainties of earlier work, was obtained (Table 1). For a pro-crystal made of neutral Mg and O atoms and $a = 4.2115$ Å, one finds, from (9) and (14*b*) (see Appendix *B* for details), $\Phi_0 = 18.43$ V.

Although MgO has been the subject of many theoretical studies, the only one we have found that reports data suitable for the evaluation of $\Phi_0$ is that of Boyer (1983). In his work, Boyer fitted the calculated self-consistent muffin-tin electron density to a sum of spherical pseudo-ions, $Mg^{2+}$ and $O^{2-}$, described by Slater-type orbitals. From these data we calculate, again from (14*b*), $\Phi_0 = 12.85$ V, in excellent agreement with experiment.

It should be remarked that the decomposition of the electron density into a sum of pseudo-atom densities is not unique. Boyer could presumably have fitted his calculated electron densities to a sum of *neutral* pseudo-atoms and it is certainly not correct to suppose that the observed $\Phi_0$ supports a completely ionic model for MgO. However, the large difference between the pro-crystal value of $\Phi_0$ and the experimental one does illustrate that $\Phi_0$ is remarkably sensitive to bonding effects.

To put the last point into perspective and to illustrate the power of electron-diffraction methods to probe bonding in crystals, we quote Zuo, Foley, O'Keeffe & Spence (1989) for the difference between the crystal and the pro-crystal: $\Delta V_{000} = 26\%$, $\Delta F_{000} = 0\%$, $\Delta V_{111} = 44\%$, $\Delta F_{111} = 12\%$, $\Delta V_{200} = 2\%$, $\Delta F_{200} = 1\%$.

### *Silicon*

Undoubtedly the most accurate set of X-ray structure factors that currently exists is for crystalline silicon. The most recent refinement (Deutsch, 1991) of the experimental data (Cummings & Hart, 1988), using an eight-parameter pseudo-atom and eighteen experimental structure factors, resulted in a goodness of fit of 1.2, implying that essentially all the information in the experimental data has been extracted. If $\Phi_0$ can indeed be obtained from pseudo-atom refinements of X-ray data, this example should provide an excellent proving ground. Accordingly, we now use Deutsch's data to evaluate $\Phi_0$ for silicon.

The monopole part of the electron density (this part only is relevant to an evaluation of $\Phi_0$) of the pseudo-atom is written as:

$$\rho(r) = Z\delta(r) * p_n(r) - \sum_i [\kappa_i^3 \rho_i(\kappa_i r) * p_i(r)]. \quad (31)$$

Here, the first term is the nuclear contribution and the sum is over the electron shells ($K$, $L$ *etc.*). In the latter, the $p_i(r)$ are normalized probability densities, $\rho_i(r)$ is the contribution of each shell to the electron density of the free atom and the $\kappa_i$ are fitted parameters to allow for expansion ($\kappa_i < 1$) or contraction ($\kappa_i > 1$) of the shell. In the harmonic approximation (which was found to apply for silicon), the Fourier transform of the probability density is $\exp(-Bk^2/4)$. The corresponding value of $v(0)$ is

$$v(0) = (2\pi/3)\sum_i (z_i \langle r^2 \rangle_{i0}/\kappa_i^2) - (ZB_n/4\pi) + \sum_i z_i B_i/4\pi. \quad (32)$$

Here, $z_i$ is the charge in units of $e$ in each shell ($2e$, $8e$ and $4e$, respectively, for silicon) and $\langle r^2 \rangle_{i0}$ is the average value of $r^2$ in each shell of the free atom.

In Deutsch's (1991) best fit [his model (*e*)], two separate harmonic temperature factors were refined. The first, $B_1 = B_2 = 0.4585\ (11)$ Å$^2$, applied to the $K$- and $L$-shell electrons; the second, $B_3 = 0(0.11)$ Å$^2$, applied to the $M$ (valence) shell. We assume that $B_1$ also applies to the nucleus ($B_n = B_1$). The other relevant parameters determined are $\kappa_1 = 1$ (assumed), $\kappa_2 = 0.9949\ (6)$, $\kappa_3 = 0.9382\ (15)$. We use a cubic lattice parameter of $a = 5.4310$ Å and find from (32) $\Phi_0 = 8v(0)/\Omega = 15.19\ (5)$ V. The contribution from the last two terms (involving the thermal parameters) is $-0.11\ (3)$ V. Note that, in the rigid-atom approximation (all $B_i = B_n$), the temperature factor does not influence $\Phi_0$.

The main difference, as far as $v(0)$ is concerned, between the atom and the pseudo-atom is due to the expansion of the valence shell by about 6%. The effect of this expansion is shown in Table 2. The same expansion has been reported in previous analyses (Aldred & Hart, 1973; Price, Maslen & Mair, 1978; Spackman, 1986) of the experimental data in terms of pseudo-atoms.

In contrast to the value of $\Phi_0 = 15.2$ V calculated from the pseudo-atom parameters, the most reliable experimental value, which includes corrections for multiple scattering, is (Table 1) 9.26 V – a spectacular disagreement.

Recall that essentially all the difference $\Phi_0 - \Phi_0$(atom) comes from the apparent expansion of the valence shell.* On the other hand, the measured value of 9.3 V would require a large *contraction* of the valence shell. We believe that the apparent expansion of the valence shell is an artifact of the particular method (length scaling) used to fit the experimental data, and that this is the Achilles' heel of this particular approach to pseudo-atom refinement. This belief is reinforced by examination of theoretical results for aluminium metal, which we discuss next. We return to a further discussion of silicon in §6.

* An earlier measurement of $\Phi_0 = 11.5\ (10)$ V for Si (Gaukler & Schwarzer, 1971) also indicates a valence-shell contraction.

Table 2. *Contributions* (*in* V) *by shell to the average Coulomb potential in silicon calculated from the pseudo-atom refinement of Deutsch* (1991)

| | $K$ | $L$ | $M$ | Total | + Thermal term |
|---|---|---|---|---|---|
| Free atom | 0.014 | 1.228 | 12.360 | 13.603 | |
| Pseudo-atom | 0.014 | 1.241 (2) | 14.042 (44) | 15.30 (4) | 15.19 (3) |

*Aluminium*

There have been at least two recent theoretical studies of metallic aluminium that have a bearing on the question of $\Phi_0$. Finnis (1990) modeled a pseudo-atom valence electron density by scaling the free-atom valence shell by a two-parameter contraction function $S(r)$:

$$S(r) = A/\{\exp[\beta(r - r_c)] + 1\}. \quad (33)$$

Here, $A$ is a normalizing constant determined by $\beta$ and $r_c$. In the limit of large $\beta$, this function corresponds to truncation of the valence shell at $r_c$, a procedure well established and tested for solids by electronic-structure theorists (*e.g.* Sankey & Niklewski, 1989). The parameters in (33) were determined from a comparison with first-principles electronic-structure calculations [for details see Finnis (1990)].

A related, but independent, theoretical investigation was recently reported by Chetty, Stokbro, Jacobsen & Nørskov (1992). These authors used pseudo-atom form factors made to fit calculated structure factors using a technique that allowed them to estimate low $k$ values and reported an analytical (five-parameter) fit to the difference $\delta f$ between the pseudo-atom and free-atom form factors.

From the data presented in the above studies, we can calculate the difference, $\delta\Phi_0$, between $\Phi_0$ for the crystal and for the pro-crystal constructed of free atoms. Remarkably, within the precision of the reported parameters, the same value is obtained in both instances and we find $\Phi_0$(pro-crystal) = 17.0 V, $\Phi_0$(crystal) = 12.7 V. Measured values for the crystal range from 11.9 to 13.0 V (Spence, 1993), in satisfactory agreement.

In Fig. 8, we show $\delta f$ for the models of Finnis (1990) and Chetty *et al.* (1992) as functions of $k$. Notice the excellent agreement in the neighborhood of $k = 0$. Also shown on the graph (points) are values

of $\delta f$ for the lowest-order reflections of aluminium assuming that the Chetty *et al.* (1992) data are correct (we emphasize that these are not experimental data). If one were to attempt to fit these points using a scaled atomic valence distribution, one would have to use an expanded atom ($\kappa < 1$), as also shown on the figure. Most importantly, the scaled electron distribution approaches $k = 0$ from the wrong side and predicts an increase (rather than a decrease) in $\Phi_0$ over the pro-crystal value [recall that $\delta v(0)$, and hence $\delta\Phi_0$, is proportional to the negative of the curvature of $\delta f(k)$ at the origin, from (10)].

Fig. 9 shows the corresponding direct-space representation of the same data given as radial distributions $R(r) = 4\pi r^2 \delta\rho(r)$. Notice the opposite behavior of the expanded atom ($\kappa = 0.9$) and the Finnis (1990) and Chetty *et al.* (1992) models and the complicated behavior near the origin, which is the most important region for $k \neq 0$ diffraction.

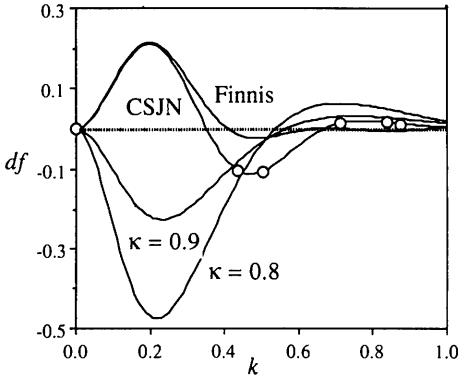


Fig. 8. The difference in form factor (pseudo-atom minus atom in units of e) for aluminium from the theoretical data of Finnis (1990) and Chetty *et al.* (1992) (CSJN) as a function of $k$ (Å$^{-1}$). The open circles mark positions of structure factors for f.c.c. metallic aluminium starting from the left with 111 (see text). The curves marked $\kappa = 0.9$ and $\kappa = 0.8$ are for pseudo-atoms constructed from length-scaled atoms.

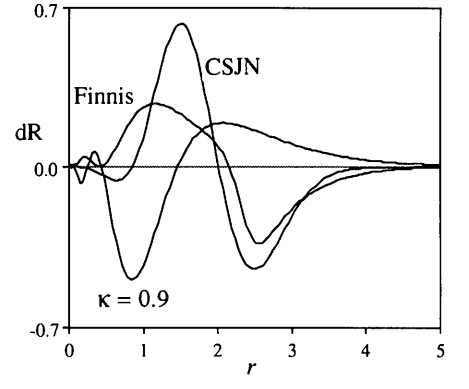


Fig. 9. The same functions as in Fig. 8, shown as radial distributions $R(r) = 4\pi r^2 \delta\rho(r)$ in direct space. Units are $R$ in e Å$^{-1}$ and $r$ in Å.

It is also rewarding to examine the ratio of the pseudo-atom and free-atom valence-electron densities shown in Fig. 10. Close to the nucleus, this is a rather complicated function due to the nodal structure of $3s$ and $3p$ wave functions [the Finnis (1990) function is, of course, uniformly smooth and the ratio is just $S(r)$ in (33)]. We find the Chetty *et al.* (1992) curve very suggestive. Electron density is removed from both the outer parts of the atom (reducing $\Phi_0$) and near the origin (reducing low-order structure factors), and 'bunched' in between. We propose that a function that plays such a rôle might be appropriate for pseudo-atom refinements of structure factors in which $\Phi_0$ is included as an additional observation. A suitable two-parameter function might be $S(r) = A/(1 - br + cr^2)$, with $b$ and $c$ adjustable parameters and $A$ a normalizing factor.

## 6. The information about $\Phi_0$ in silicon structure factors

Structure factors for silicon have been the subject of innumerable theoretical and experimental investigations, with recent contributions representing the current state of the art for both aspects. Here we assess the information content of the experimental data and the relevance of theoretical calculations. The experimental data to which we will refer are those summarized by Cummings & Hart (1988), together with the 'forbidden' 222 structure factor (Alkire, Yelon & Schneider, 1982). These 18 data, which have estimated standard deviations of 1–5 $\times 10^{-3}$ e atom$^{-1}$ are listed in Table 1 of Lu & Zunger (1992).

Early theoretical electronic structure studies of crystalline silicon were summarized by Spackman (1986), who pointed out that these typically gave $R$

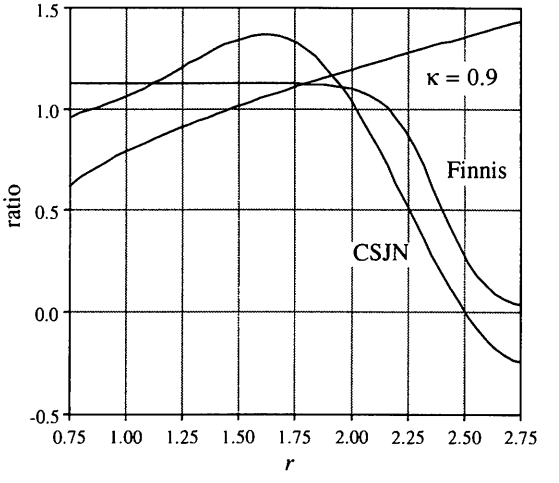


Fig. 10. The ratio of the electron density of the pseudo-atoms of Figs. 8 and 9 to the free-atom electron density for aluminium as a function of distance from the nucleus ($r$ in Å).

= 1% where $R = \Sigma||F_{obs}| - |F_{calc}||/\Sigma|F_{obs}|$. To put this in perspective, we note that, for the 18 $F$ mentioned above and using a pro-crystal of Hartree–Fock *atoms* (Clementi & Roetti, 1974) to calculate structure factors, we obtain $R = 0.76\%$, so that the pro-crystal is a better approximation to the real crystal than the calculated ones.

Recently, Lu & Zunger (1992) have reported what is possibly the most accurate electronic structure calculation for crystalline silicon to date; this results in $R = 0.21\%$, a very significant improvement. However they argue that the finer details of the electron distribution can only be revealed from a Fourier synthesis that involves a very large number of terms and this claim needs careful evaluation. Lu and Zunger's calculated structure factors differ from the experimental data by as many as 20 standard deviations for the crucial low-order reflections, presumably owing to approximations made in the calculations. If the first four structure factors (111, 220, 311 and 222) are excluded, their $R$ is 0.23% and that for the Hartree–Fock pro-crystal is 0.27%, so, on an absolute basis, the pro-crystal is virtually equivalent to the calculated one for the higher orders. However, interest usually focuses on deformation density obtained from a synthesis of $F_{crystal} - F_{pro\text{-}crystal}$. If the systematic errors in theoretical calculations (which are very precise, if not very accurate compared to measurement) largely cancel each other out, then fine detail in high-order syntheses may be significant, but this remains to be demonstrated in a rigorous manner.

It is also important to keep in perspective the practical realities. In Fig. 11, we show the difference in the calculated structure factors (Lu & Zunger, 1992) for the crystal and the pro-crystal, $DF$ ($= F_{calc} - F_{sup}$ in Lu & Zunger's notation), as a function of $H$. It may be seen that the difference is less than $3 \times 10^{-3}$ e atom$^{-1}$ after 12 reflections. As experimental data are subject to errors of at least this magnitude, it should be clear that *experimental* data beyond this point contain no information about the electron redistribution after bonding and will only contribute noise to deformation-density maps (they do, of course, contain valuable information about thermal parameters). The same conclusion was reached on the basis of an error analysis of silicon deformation-density maps by Maslen (1988), and in a slightly different context by Zuo, Spence & O'Keeffe (1988, 1989).

The deformation density in silicon is determined from a Fourier synthesis of $\Delta F = F - F_{atom}$, where $F$ is the measured structure factor and $F_{atom}$ refers to the pro-crystal. Let us further write $F = F_{sp} + F_{ns}$, where $F_{sp}$ is the contribution from the spherical part of the fitted pseudo-atom and $F_{ns}$ is that from the non-spherical part. Again using Deutsch's (1991) fit, it is found that $F_{sp} - F_{atom}$ (in $10^{-3}$ e atom$^{-1}$) are 111: −181; 220: −72; 311: −32; 220: 0; 400: −2; 331: 2. Thus, essentially, only the first three reflections give information about how the radial part of the pseudo-atom differs from the free atom. This is in accordance with Lu & Zunger's (1992) observation that a synthesis of $F_{ns}$ already gives the essential details of the deformation density in the valence region (including the peak height in the mid-bond region).

We conclude, therefore, that for silicon only about 12 experimental structure factors give information about the differences between pseudo-atom electron densities and those of free atoms, and that only a small part of these structure factors gives information about the radial part of this difference. Thus, only one parameter can be realistically refined for this part from X-ray data. For other materials, with less-accurate structure factors available, the situation is even more restricted.

In Fig. 12, we show the contributions to $f(H)$ of the various shells of the Clementi & Roetti (1974) silicon atom. Recall (10), which shows that $v(0)$ (and hence $\Phi_0$) is determined by the curvature of $f(k)$ at the origin. The figure illustrates that, as is well known, the valence electrons contribute mainly to the small $k$ part but also that they dominate the curvature at $k = 0$. Confronted with just the points presented in the figure, one would conclude that anything more than an order-of-magnitude estimate of this curvature was impossible. The data also show that attempting to refine $s$ and $p$ populations is unlikely to be useful.

In the light of the above remarks, it should be clear that $\Phi_0$, as measured by electron diffraction, provides important extra information about the radial part of the valence electron density that is not available from X-ray diffraction data. In particular,

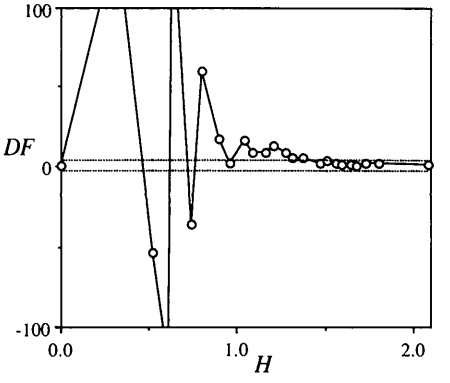


Fig. 11. DF = the difference between calculated (Lu & Zunger, 1992) structure factors (in $10^{-3}$ e atom$^{-1}$) for crystalline silicon and for free atoms as a function of $H$ (in Å$^{-1}$). The dotted lines are at $\pm 3 \times 10^{-3}$ e. Note that three points fall outside the range of the graph.

a two-parameter fit of the radial part of the valence electron density of silicon should be possible with the additional observation provided by $\Phi_0$. Note that this extra information does not come from high-order structure factors but from information at $\mathbf{H} = \mathbf{0}$.

## 7. Concluding remarks

With recent developments in electron holography (Tonomura, 1987) and of methods for properly taking into account dynamical effects in electron diffraction (Spence & Zuo, 1992), it is anticipated that accurate values of $\Phi_0$ will soon be available for a variety of materials. We note that possible effects of surface dipole layers must be carefully evaluated; indeed, in appropriate systems with deliberately adsorbed surface layers, measurements of $\Phi_0$ could be used to determine the density and sign of surface dipoles.

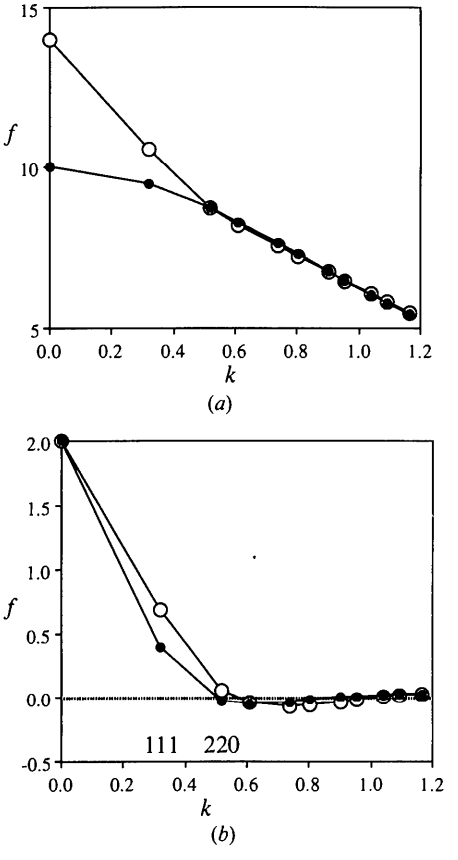


Fig. 12. The form factor (in e atom$^{-1}$) for the Clementi & Roetti (1974) Si atom at points corresponding to reciprocal-lattice vectors of crystalline silicon as a function of $H$ (in Å$^{-1}$). In (*a*), open circles represent the total and filled circles the core contribution. In (*b*), open circles represent the 3*s* contribution and filled circles the 3*p* contribution.

The examples we have considered show that $\Phi_0$ is very sensitive to bonding effects in crystals and provides a stringent constraint of model valence-electron densities. We urge electronic-structure theorists who calculate structure factors to include $V(0)$ (and hence $\Phi_0$) in their considerations as it will provide powerful tests of both theory and experiment which are so far lacking.

We note that, in all cases where accurate values are available, $\Phi_0$ is less than the pro-crystal value. This suggests that as a general rule the valence-electron density is *contracted* when atoms combine to form crystals.

Finally, we conclude that it is not possible (when confronted with the reality of experimental uncertainties) to get reliable information about the missing $V(0)$ from measured $F(\mathbf{H})$ [or $V(\mathbf{H})$] for nonzero $\mathbf{H}$. The implication is that diffraction data do not give all the information about valence-electron distributions that is available when the data are supplemented with knowledge of $\Phi_0$. Therefore, we suggest that future pseudo-atom refinements use the measured value of $\Phi_0$ as an additional observation when it is available (as for silicon).

This work was supported by a grant (DMR 90 15867) from the US National Science Foundation. We are pleased to acknowledge useful and stimulating discussions with many colleagues, particularly J. M. Cowley, P. Rez, O. F. Sankey and J. M. Zuo. We are grateful to M. A. Spackman for calling our attention to some key references and for helpful comments on an earlier version of the manuscript.

## APPENDIX *A*

### A note on sum rules for structure factors

Substitution of (22) for $\rho(\mathbf{r})$ in (16*a*) gives, for a crystal with pseudo-atoms at the points of a simple cubic lattice,

$$\Phi_{01} = (-2\pi/3\Omega^2)\sum_{\mathbf{H}} f_a(\mathbf{H}) \int_{\text{cell}} r^2 \exp(-2\pi i \mathbf{H}\cdot\mathbf{r})\mathrm{d}\mathbf{r}. \qquad (A1)$$

The value of the integral in this expression must be determined using the same origin as is used for the structure factor.

We take the origin on the atom and integrate over the range $-a/2 \le x,y,z \le a/2$. The value of the integral is $(-1)^h a^5/2\pi^2 h^2$ for $\mathbf{H} = h\mathbf{a}^*$ or $h\mathbf{b}^*$ or $h\mathbf{c}^*$ ($h$ an integer) and zero otherwise, and

$$\Phi_{01} = (-2/\pi a)\sum_{1}^{\infty}(-1)^h f_a(h,0,0)/h^2. \qquad (A2)$$

This is just a special case of the more general sum rule given by equation (48) of Becker & Coppens (1990). We saw in Fig. 2 that, in the limit of a large unit cell, $\Omega\Phi_{01} = \Omega\Phi_{02} = v(0)$ for an atom. Writing $f_a(\mathbf{k}) = Z - f_{el}(\mathbf{k})$, where $Z$ is the nuclear charge and $f_{el}(\mathbf{k})$ is the electronic form factor, and using $\sum(-1)^n/n^2 = -\pi^2/12$, we get, from (*A*2), for an atom or pseudo-atom:

$$v(0) = \lim_{d\to\infty}\left((2d^2/\pi)\left\{(Z\pi^2/12) + \sum_{n=1}^{\infty}[(-1)^n f_{el}(n/d)/n^2]\right\}\right), \qquad (A3)$$

which is equivalent to Shinohara's (1932) formula for $\langle r^2\rangle$. There was at one time considerable debate (*e.g.* Miyake, 1940) about the appropriate value of $d$ to use in (*A*3). Fig. 2 answers that question.

From (4), it may be seen that (*A*3) may also be written

$$v(0) = 2\lim_{d\to\infty}\left[\sum_{n=1}^{\infty}(-1)^{n+1}v(n/d)\right]. \qquad (A4)$$

The same expression is true for a large class of functions $g(z)$ for which $g(0)$ is finite and which approach zero asymptotically. It can equally be used to get $f(0)$ from atomic form factors $f(k)$. Its historical significance (Miyake, 1940) lies in the fact that $v(0)$ is given accurately for modest $d$. In the case of a silicon atom, both $v(0)$ and $f(0)$ are given to better than 1% for $d = 6$ Å. In general, functions for which $g(\mathrm{d}^2g/\mathrm{d}z^2)$ is negative when $|g|$ is large have this property of rapid convergence to the limit with $d$. Note that the electron density $\rho(r)$ and Coulomb potential $\varphi(r)$ for an atom are not examples of such functions.

In contrast, the Becker & Coppens sum rule [equation (48) of Becker & Coppens (1990)] is an exact rule for sums on $v(k)$ yielding $\Phi_{01}$ (a well defined quantity) for a definite choice of $d$ (the unit-cell edge). We remark that the same difficulties attend on obtaining $\Phi_{01}$ from X-ray diffraction data as on obtaining $\Phi_0$.

## APPENDIX *B*

### Use of Slater-type orbitals to obtain $v(k)$ for small $k$

Difficulties in the practical determination of $v(k)$ for atoms when $k$ is small were recently discussed by Peng & Cowley (1988). For atomic wave functions described by Slater-type orbitals, the procedure is straightforward. Continuing the expansion (7) of $v(k)$ for a spherical atom, we get

$$v(k) = (2\pi Z\langle r^2\rangle/3) - (Z/\pi) \times \sum_{n=2}^{\infty}[(-1)^n(2\pi)^{2n}\langle r^{2n}\rangle k^{2n-2}/(2n+1)!]. \qquad (B1)$$

A spherically averaged atomic orbital expressed as a sum of Slater-type orbitals is

$$\varphi_p = \sum_i A_{pi}R_{pi}, \qquad (B2)$$

where

$$R_{pi} = r^{n_{pi}-1}\exp(-\zeta_{pi}r), \qquad (B3)$$

$$A_{pi} = (1/2\pi^{1/2})c_{pi}[(2n_{pi})!]^{-1/2}(2\zeta_{pi})^{n_{pi}+1/2}. \qquad (B4)$$

Values of $n_{pi}$, $c_{pi}$ and $\zeta_{pi}$ for atoms and some ions with $Z \le 54$ are given by Clementi & Roetti (1974).

Let the occupancy of the $p$th orbital be $o_p$ and $A_{pij} = A_{pi}A_{pj}$, $\zeta_{pij} = \zeta_{pi} + \zeta_{pj}$ and $n_{pij} = n_{pi} + n_{pj}$. Then,

$$Z\langle r^m\rangle = 4\pi\sum_p o_p\sum_i\sum_j A_{pij}[(n_{pij}+m)!/\zeta_{pij}^{n_{pij}+m+1}]. \qquad (B5)$$

The use of a minimal set of Slater-type functions with one exponent per orbital ('single zeta') is inadequate to determine $v(0)$. For silicon, the Hartree–Fock wave function of Clementi & Roetti (1974) gives $v(0) = 272.4$ V Å$^3$; the single-zeta wave function of the same authors yields $v(0) = 236.8$ V Å$^3$. The value calculated from the electron scattering factor for silicon, $f^B(0) = 5.828$ Å, in *International Tables for Crystallography* (Cowley, 1992) is $v(0) = 5.828 \times 47.88 = 279.0$ V Å$^3$.

### References


ALDRED, P. J. E. & HART, M. (1973). *Proc. R. Soc. London Ser. A*, **332**, 223–228.

ALKIRE, R. W., YELON, W. B. & SCHNEIDER, J. R. (1982). *Phys. Rev. B*, **26**, 3097–3104.

BECKER, P. & COPPENS, P. (1990). *Acta Cryst.* A**46**, 254–258.

BETHE, H. A. (1928). *Ann. Phys. (Leipzig)* **87**, 55–128.

BOYER, L. L. (1983). *Phys. Rev. B*, **27**, 1271–1275.

CHANG, S.-L. (1987). *Crystallogr. Rev.* **1**, 87–149.

CHETTY, N., STOKBRO, K., JACOBSEN, K. W. & NØRSKOV, J. K. (1992). *Phys. Rev. B*, **46**, 3798–3809.

CLEMENTI, E. & ROETTI, C. (1974). *At. Data Nucl. Data Tables*, **14**, 177–478.

COWLEY, J. M. (1992). In *International Tables for Crystallography*, Vol. C, edited by A. J. C. WILSON. Dordrecht: Kluwer Academic Publishers.

CUMMINGS, S. & HART, M. (1988). *Aust. J. Phys.* **41**, 423–431.

DAVISSON, C. J. & GERMER, L. H. (1927). *Phys. Rev.* **30**, 705–715.

DAWSON, B. (1967). *Proc. R. Soc. London Ser A*, **298**, 255–263.

DEUTSCH, M. (1991). *Phys. Lett.* A**153**, 368–372.

EWALD, P. P. & JURETSCHKE, H. (1953). In *Structure and Properties of Solid Surfaces*, edited by R. GOMER & C. S. SMITH. Univ. of Chicago Press.

FINNIS, M. W. (1990). *J. Phys. Condens. Mat.* **2**, 331–342.

FUCHS, K. (1935). *Proc. R. Soc. London Ser. A*, **151**, 585–595.

GAJDARDZISKA-JOSIFOVSKA, M., MCCARTNEY, M. R., DE RUIJTER, W. J., SMITH, D. J., WEISS, J. K. & ZUO, J. M. (1993). *Ultramicroscopy*. In the press.

GAUKLER, K. H. & SCHWARZER, R. (1971). *Optik (Weimar)*, **33**, 215–237.

HANSEN, N. K. & COPPENS, P. (1978). *Acta Cryst.* A**34**, 909–921.

HARRIS, F. E. (1975). *Theoretical Chemistry, Advances and Perspectives*, edited by H. EYRING & D. HENDERSON, Vol. 1, pp. 147–218. New York: Academic.

IBERS, J. A. (1958). *Acta Cryst.* **11**, 178–183.

JACKSON, J. D. (1975). *Classical Electrodynamics*, 2nd ed. New York: Wiley.
JONA, F. & SHIRANE, G. (1962). *Ferroelectric Crystals*. New York: Pergamon.
KISLIUK, P. (1961). *Phys. Rev.* **122**, 405–417.
KLEINMAN, L. (1981). *Phys. Rev. B*, **24**, 7412–7414.
LANG, N. D. & KOHN, W. (1971). *Phys. Rev. B*, **3**, 1215–1228.
LASCHKAREW, W. E. & TSCHABAN, A. S. (1935). *Phys. Z Sowjetunion*, **8**, 240–254.
LAUE, M. VON (1948). *Materiewellen und ihre Interferenze*. Leipzig: Geest & Portig.
LU, Z. W. & ZUNGER, A. (1992). *Acta Cryst.* A**48**, 545–554.
MASLEN, E. N. (1988). *Acta Cryst.* A**44**, 33–37.
MIYAKE, S. (1940). *Proc. Phys. Math. Soc Jpn*, **22**, 666–676.
PENG, L.-M. & COWLEY, J. M. (1988). *Acta Cryst.* A**44**, 1–5.
PRICE, P. F., MASLEN, E. N. & MAIR, S. L. (1978). *Acta Cryst.* A**34**, 183–193.
REZ, P. (1978). *Acta Cryst.* A**34**, 48–51.
ROSENFELD, L. (1929). *Naturwissenschaften*, **17**, 49–50.
SANKEY, O. F. & NIKLEWSKI, D. J. (1989). *Phys. Rev. B*, **40**, 3979–3995.
SAUNDERS, V. R., FREYRIA-FAVA, C., DOVESI, R., SALASCO, L. & ROETTI, C. (1992). *Mol. Phys.* **77**, 629–665.
SHINOHARA, K. (1932). *Sci. Pap. Inst. Phys. Chem. Res. Tokyo*, **18**, 315–319.
SPACKMAN, M. A. (1986). *Acta Cryst.* A**42**, 271–281.
SPACKMAN, M. A. & STEWART, R. F. (1981). *Chemical Applications of Atomic and Molecular Electrostatic Potentials*, edited by P. POLITZER & D. G. TRUHLAR, pp. 407–425. New York: Plenum.
SPENCE, J. C. H. (1993). *Acta Cryst.* A**49**, 231–260.
SPENCE, J. C. H. & ZUO, J. M. (1992). *Electron Microdiffraction*. New York: Plenum.
STERN, R. M. & GERVAIS, A. (1969). *Surf. Sci.* **17**, 273–301.
STEWART, R. F. (1973). *J. Chem. Phys.* **58**, 1668–1676.
TAMM, I. (1932). *Phys. Rev.* **39**, 170–173.
THOMSON, G. P. & COCHRANE, W. (1939). *Theory and Practice of Electron Diffraction*. London: Macmillan.
THOMSON, G. P. & REID, A. (1927). *Nature (London)*, **119**, 890–895.
TONOMURA, A. (1987). *Rev. Mod. Phys.* **59**, 639–693.
TOSI, M. P. (1964). *Solid State Phys.* **16**, 1–120.
YADA, K., SHIBATA, K. & HIBI, T. (1973). *J. Electron Microsc.* **22**, 223–230.
YOSHIOKA, H. (1957). *J. Phys. Soc. Jpn*, **12**, 618–630.
ZUO, J. M., FOLEY, J. A., O'KEEFFE, M. & SPENCE, J. C. H. (1989). *Metal-Ceramic Interfaces*, edited by M. RUHLE, pp. 45–51. New York: Pergamon.
ZUO, J. M., SPENCE, J. C. H. & O'KEEFFE, M. (1988). *Phys. Rev. Lett.* **61**, 353–356.
ZUO, J. M., SPENCE, J. C. H. & O'KEEFFE, M. (1989). *Phys. Rev. Lett.* **62**, 2329.

*Acta Cryst.* (1994). A**50**, 45–52

# The Calculation of Scattering Factors in HREM Image Simulation

BY D. TANG AND D. DORIGNAC

*CEMES-LOE/CNRS, BP*4347, 31055 *Toulouse CEDEX, France*

(*Received* 14 *December* 1992; *accepted* 3 *June* 1993)

## Abstract

Two analytical approximations currently used for evaluating scattering factors for electrons, from a relativistic Hartree–Fock atomic potential and following the first Born approximation, are systematically studied. It is shown that their deviations from the scattering factors directly derived from the numerical Fourier transform of the potential vary with the spatial frequency and that these deviations are sufficiently large to introduce perceptible differences in the simulated image features, especially when strong multiple scattering occurs. In order to use better scattering factors and improve image interpretation, a new simple method combining both analytical approximations is suggested. For the first time, a more sophisticated atomic potential, a relativistic Hartree–Fock–Slater model, is also considered in the calculations. The importance of using accurate scattering factors in HREM image simulation is pointed out, particularly for future quantitative microscopy with the new ultra high resolution electron microscopes.

## Introduction

In high-resolution electron microscopy (HREM), the calculation of atomic scattering factors for electrons is required for the interpretation of the images, which is based on comparison with computer simulations. The routine calculation is based on an analytical approximation: the scattering-factor curve is fitted to sums of several Gaussian functions of the form

$$f(g) = \sum_{i=1}^{n} a_i \exp(-b_i g^2/4) + c, \qquad (1)$$

where the coefficients $a_i$, $b_i$ and $c$ differ from one atom to another and $g$ is the spatial frequency. With suitable scaling of the corresponding coefficients, $f(g)$ may be the scattering factor for electrons ($f_e$) or for X-rays ($f_x$) (Vand, Eiland & Pepinsky, 1957; Smith &